ISSN 1063-7788, Physics of Atomic Nuclei, 2018, Vol. 81, No. 9, pp. 1294–1300. © Pleiades Publishing, Ltd., 2018.
Original Russian Text © A.Sh.M. Elshoukrofy, E.B. Postnikov, I.I. Astapov, P.A. Bezyazeekov, V. Boreyko, A.N. Borodin, N.M. Budnev, R. Wischnewski, A.Y. Garmash, A.R. Gafarov, N.V. Gorbunov, V.M. Grebenyuk, O.A. Gress, T.I. Gress, A.A. Grinyuk, O.G. Grishin, A.N. Dyachok, A.V. Zagorodnikov, V.L. Zurbanov, A.L. Ivanova, Y.A. Kazarina, N.N. Kalmykov, N.I. Karpov, V.V. Kindin, P.S. Kirilenko, S.N. Kiryuhin, V.A. Kozhin, R.P. Kokoulin, K.G. Kompaniets, E.E. Korosteleva, E.A. Kravchenko, L.A. Kuzmichev, M. Kunnas, A. Chiavassa, A.A. Lagutin, V.V. Lenok, B.K. Lubsandorzhiev, N.B. Lubsandorzhiev, R.R. Mirgazov, R. Mirzoyan, R.D. Monkhoev, H.A. Motaweh, R. Nachtigall, E.A. Osipova, M.I. Panasyuk, L.V. Pankov, A.L. Pakhorukov, A.A. Petrukhin, V.A. Poleschuk, M. Popesku, E.G. Popova, A. Porelli, V.V. Prosin, V.S. Ptuskin, A.A. Pushnin, R.I. Raikin, G.I. Rubtsov, Ya.I. Sagan, V.S. Samoliga, L.G. Sveshnikova, Yu.A. Semeney, A.Y. Sidorenkov, A.A. Silaev, A.A. Silaev Jr., A.V. Skurikhin, M. Slunecka, A.V. Sokolov, V.P. Sulakov, V.A. Tabolenko, B.A. Tarashansky, L.G. Tkachev, A.V. Tkachenko, M. Tluczykont, O.L. Fedorov, D. Horns, C. Spiering, I.I. Yashin, 2017, published in Yadernaya Fizika i Inzhiniring, 2017, Vol. 8, No. 4, pp. 311–318.

MATHEMATICAL MODELING IN NUCLEAR TECHNOLOGIES

Application of New Approximations of the Lateral Distribution of EAS Cherenkov Light in the Atmosphere

A. Sh. M. Elshoukrofy[a, b], E. B. Postnikov[a, *], I. I. Astapov[c], P. A. Bezyazeekov[d], V. Boreyko[e], A. N. Borodin [e], N. M. Budnev[d], R. Wischnewski[f], A. Y. Garmash[g, h], A. R. Gafarov[d], N. V. Gorbunov[e], V. M. Grebenyuk [e], O. A. Gress[d], T. I. Gress[d], A. A. Grinyuk[e], O. G. Grishin[d], A. N. Dyachok[d], A. V. Zagorodnikov[d], V. L. Zurbanov[d], A. L. Ivanova[d], Y. A. Kazarina[d], N. N. Kalmykov[a], N. I. Karpov[a], V. V. Kindin[c], P. S. Kirilenko[g], S. N. Kiryuhin[d], V. A. Kozhin[a], R. P. Kokoulin[c], K. G. Kompaniets[c], E. E. Korosteleva[a], E. A. Kravchenko[g, h], L. A. Kuzmichev[a, d], M. Kunnas[i], A. Chiavassa[j, k], , A. A. Lagutin[l], V. V. Lenok[d], B. K. Lubsandorzhiev[m], N. B. Lubsandorzhiev[a], R. R. Mirgazov[d], R. Mirzoyan[n], R. D. Monkhoev[d], H. A. Motaweh[b], R. Nachtigall[h], E. A. Osipova[a], M. I. Panasyuk[a], L. V. Pankov[d], A. L. Pakhorukov[d], A. A. Petrukhin[c], V. A. Poleschuk[d], M. Popesku[o], E. G. Popova[a], A. Porelli[f], V. V. Prosin[a], V. S. Ptuskin[p], A. A. Pushnin[d], R. I. Raikin[l], G. I. Rubtsov[m], Ya. I. Sagan[e], V. S. Samoliga[d], L. G. Sveshnikova[a], Yu. A. Semeney[d], A. Y. Sidorenkov[m], A. A. Silaev[a], A. A. Silaev Jr.[a], A. V. Skurikhin[a], M. Slunecka[e], A. V. Sokolov[g, h], V. P. Sulakov[a], V. A. Tabolenko[d], B. A. Tarashansky[d], L. G. Tkachev[e], A. V. Tkachenko[e], M. Tluczykont[i], O. L. Fedorov[d], D. Horns[i], C. Spiering[f], and I. I. Yashin[c]

[a] *Skobeltsyn Institute of Nuclear Physics, Moscow State University, Moscow, 119991 Russia*
[b] *Damanhour University, Damanhour, Egypt*
[c] *National Research Nuclear University MEPhI (Moscow Engineering Physics Institute), Moscow, 115409 Russia*
[d] *Research Institute of Applied Physics, Irkutsk State Universiry, Irkutsk, 664020 Russia*
[e] *Joint Institute for Nuclear Research, Dubna, Moscow oblast, 141980 Russia*
[f] *Deutsches Elektronen-Synchrotron DESY, Zeuthen, D-15738 Germany*
[g] *Novosibirsk State University, Novosibirsk, 630090 Russia*
[h] *Budker Institute of Nuclear Physics, Siberian Branch, Russian Academy of Sciences, Novosibirsk, 630090 Russia*
[i] *Institut für Experimentalphysik, Universität Hamburg, D-22761 Hamburg, Germany*
[j] *Physics Department, University of Torino, Turin, 10125 Italy*
[k] *National Institute of Nuclear Physics INFN, Turin, 10125 Italy*
[l] *Altai State University, Barnaul, 656049 Russia*
[m] *Institute for Nuclear Research, Russian Academy of Sciences, Moscow, 117312 Russia*
[n] *Max Planck Institute for Physics, München, D-80805 Germany*
[o] *Institute of Space Science, Bucharest, 050107 Romania*
[p] *Pushkov Institute of Terrestrial Magnetism, Ionosphere, and Radio Wave Propagation, Russian Academy of Sciences, Troitsk, Moscow oblast, 108840 Russia*
**e-mail: evgeny.post@gmail.com*

Received September 21, 2017

Abstract—A new knee-like approximation of the lateral distribution function (LDF) of EAS Cherenkov light in the 30–3000 TeV energy range was proposed and tested with simulated showers in our earlier studies. This approximation fits the LDFs of individual showers accurately for all types of primary particles gamma-rays, protons, and nuclei) and is suitable for reconstructing the shower core, determining the energy, and separating gamma-induced showers from hadron-induced ones. In the present study, the knee-like fitting function is used to determine the parameters of real showers detected by TAIGA-HiSCORE. It is demonstrated that this approximation characterizes properly all types of individual LDFs of experimental events in the 300–1000 TeV range. The accuracy of fit is governed by fluctuations intrinsic to the process of measurement of the Cherenkov photon density. The probability density function of these fluctuations was reconstructed and introduced into simulations. Certain useful methodical applications of the knee-like approximation are considered, and the possibility of shower sorting into nuclei groups is examined. The extensive statistical coverage and detailed LDF measurement data of HiSCORE have provided the first opportunity to examine in depth the LDF of Cherenkov radiation in the 300–1000 TeV range.

Keywords: cosmic rays, EAS, Cherenkov light, primary nuclei, chemical composition

DOI: 10.1134/S1063778818090090

1. INTRODUCTION

Primary particles (cosmic rays and gamma-rays) entering the atmosphere are unable to reach ground-based detectors, since the thickness of the atmospheric layer exceeds the range of nuclear interaction by a factor of 10 or more. However, high-energy particles generate cascades of secondary particles (extensive air showers, EASs), thus producing different types of radiation that may be detected by ground-based facilities. EAS Cherenkov radiation, which is produced by secondary charged particles moving with velocities higher than the speed of light in air, is often used in such experiments. In gamma-ray astronomy, imaging atmospheric Cherenkov telescopes (IACTs) have been used since 1989 by the Whipple collaboration [1], and a number of much more sophisticated observatories (VERITAS, MAGIC, etc. [2–4]) are currently in operation. In cosmic ray physics, networks of wide-angle optical stations, which measure the Cherenkov photon density and the light front arrival time $Q_i(R, t)$, are normally used instead of IACTs. Such setups are less costly than IACTs, and their effective detection area may be larger than 10 km^2 [5–7]. The HiSCORE (High Sensitivity Cosmic ORigin Explorer) array of the TAIGA (Tunka Advanced Instrument for cosmic ray physics and Gamma-ray Astronomy) observatory [7–9] is one of the most rapidly developing facilities of this kind. It is designed to search for primary gamma-rays with energies $E > 30$–50 TeV and study the spectra and the composition of cosmic rays with $E > 100$ TeV.

Having analyzed the Cherenkov photon density and the light front arrival times, one may determine the parameters of primary particles producing the shower (specifically, their arrival direction and energy and the position of the shower core [9–11]). The determination of the particle type is a separate and difficult problem. The idea of using the differences in lateral distribution functions (LDFs) of Cherenkov radiation was proposed as a criterion for EAS sorting by particle type more than 30 years ago, when it became clear that the LDF slope is correlated with the depth of the shower maximum and, consequently, with the type of primary particles [12]. The results of our studies with simulated showers revealed that the slope and features of the shower LDF depend on several factors (energy, angle of arrival, depth of the maximum); in addition, it was demonstrated that not only the general LDF is sensitive to the type of primary particles. Therefore, the choice of fitting functions for the LDF, which should reproduce the specific features of the lateral distribution, is crucial to solving this problem. The extensive statistical coverage and detailed LDF measurement data of HiSCORE have provided the first opportunity to examine in depth the LDF of Cherenkov light in the 300–1000 TeV range and sort showers into groups of nuclei.

HiSCORE used an adapted method for reconstructing the shower parameters developed for Tunka-133 (a wide-angle nonimaging Cherenkov experiment [13]) and the 10^{16}–10^{18} eV energy range. A universal piecewise continuous function [9, 11] (Tunka fit) was constructed from four functions with their parameter set reduced to two parameters: a (normalizing factor) and bxy (LDF slope). The Tunka fit is well suited for all LDFs within its design range of 10^{15}–10^{18} eV. It also provides a close fit to the majority of LDFs in the 30–3000 TeV range; however, we have demonstrated in [14] that gamma-ray induced and nuclear showers with large (>40°) arrival angles may have a sagging shape with sharp edges, which are not reproduced by the fitting functions in question. This prompted the development of new knee-like approximations. The results of tests with Monte Carlo simulated showers [14–16] confirmed that these new functions provide a close fit to all LDF types for all primary particles with energies ranging from several tens of teraelectronvolts to petaelectronvolts. In the present study, the knee-like function is used to determine the parameters of experimental showers detected by TAIGA-HiSCORE, and the fitting accuracy and the influencing factors are examined. Certain practical applications of the knee-like approximation and the possibility of separating light nuclei from heavy ones by parametric analysis of LDFs are also considered.

2. KNEE-LIKE APPROXIMATION

The knee-like function proposed in [14] characterizes the lateral density of Cherenkov photons (i.e., the density as a function of distance to the shower core in the shower plane $Q(R)$). Function (1) depends on four parameters (γ_1, γ_2, R_0, and α) and normalizing factor C:

$$F_{\text{app}} = CR^{\gamma_1}\left(1+\left(\frac{R}{R_0}\right)^{\alpha}\right)^{\frac{\gamma_2}{\alpha}}. \tag{1}$$

Although LDFs vary greatly, all of them have a specific shape on a log-log scale and resemble the knee in the spectrum of Galactic cosmic rays, which was char-

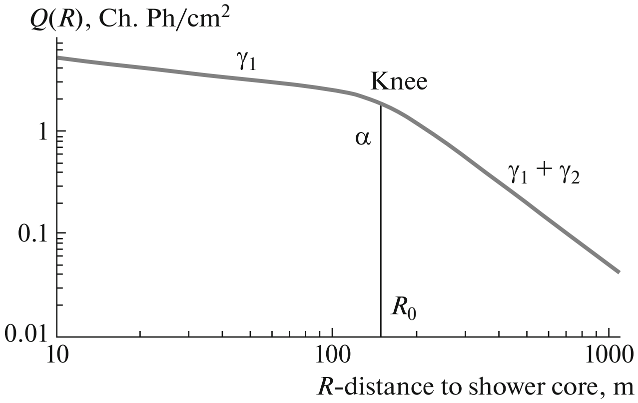

Fig. 1. Knee-like Cherenkov LDF approximation and its parameters: R_0 is the knee position, γ_1 and $\gamma_2 + \gamma_1$ are the slope factors of the power function before and after the knee, α characterizes the smoothness of the knee, and C is a normalizing factor.

acterized earlier in [17]: a disk of direct Cherenkov light $Q(R) \sim R^{\gamma_1}$ propagates to the point of the knee (R_0). Beyond R_0, $Q(R)$ also has a power-law shape $Q(R) \sim R^{\gamma_1+\gamma_2}$, but the photon density decreases greatly: $\gamma_1 + \gamma_2 \simeq 2$. This part represents the radiation produced by multiple rescattering of electrons. Parameter R_0 depends almost linearly on the distance to the depth of the maximum and falls within the range of 75–170 m [14–16]. Parameter α governs the degree of curve bending at the knee point and is the distinguishing feature of our approximation. It varies from zero to infinity and normally has a double-humped distribution, which allows one to distinguish smooth LDFs from sharp ones. The results of earlier Monte Carlo tests with simulated EASs [14–16] revealed that this function fits all individual LDFs accurately in the 30–3000 TeV energy range with zenith angles varying from 0° to 50° and R up to 600 m; the root-mean-square error is ~0.0005–0.002 on a logarithmic scale for all energies and all particle types. The parameters depend monotonically on energy and are correlated with each other. This makes it possible to reduce the number of parameters from five to three if few detectors were triggered [15]. It was demonstrated in [15, 16] that the knee-like function is suitable for reconstructing the shower core, determining the energy, and separating gamma-ray induced showers from those induced by charged particles. In the present study, we focus on the specifics of application of this function to experimental showers detected by HiSCORE.

3. APPROXIMATION OF LDFs OF EXPERIMENTAL EVENTS BY KNEE-LIKE FITTING FUNCTIONS

A sample of showers detected by TAIGA-HiSCORE on January 1 and February 1, 2017, was used. A total of 28 optical stations (each with an angle of view of 0.6 sr and an effective light-collection area of 0.5 m^2) distributed over an area of 0.25 km^2 at a pitch of 106 m were then active. Each station operates independently and detects Cherenkov pulses at a pitch of 0.5 ns, which is synchronized with all the other stations. Amplitude at maximum A_i, time T_i, and total density Q_i of Cherenkov photons, which is determined as the integral of a pulse (i.e., the area below it), are measured. A trigger signal is produced if the amplitude exceeds the average background night-sky level by 5σ. The design of the optical station, the structure of data recording and synchronization systems, and other technical details were discussed in [7–9]. The sample contains showers with a station counting rate of 16 Hz, which corresponds to cloudless and moonless nights.

The shower parameters were reconstructed in accordance with the standard HiSCORE procedure [9, 10]: the shower arrival direction (θ, φ) is first esti-

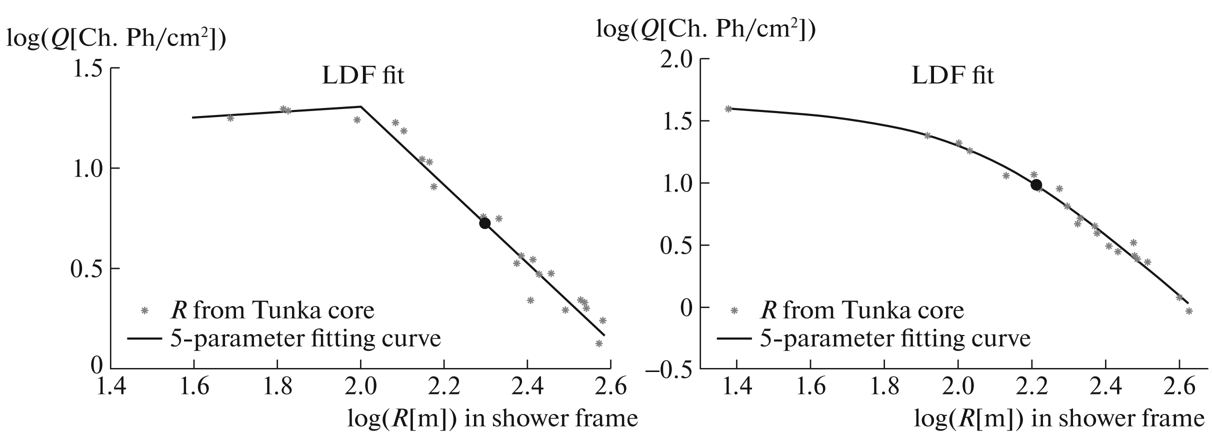

Fig. 2. Examples of experimental LDFs for two showers (small dots) and the corresponding approximating knee-like functions. Large dots correspond to the predicted densities at the IACT position (see Section 4).

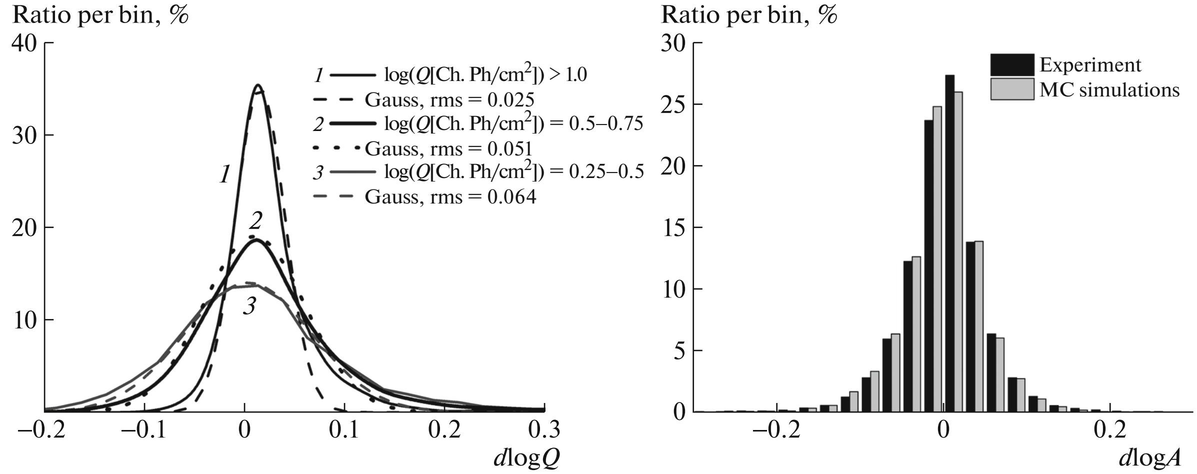

Fig. 3. Left panel: distributions of experimental deviations $d\log Q = \log Q_{\rm exp} - \log Q_{\rm fit}$ from fitting functions for three narrow Q intervals and their Gaussian approximations. Right panel: overall distributions of $d\log A$: black and gray bars correspond to experiments and Monte Carlo simulations with measurement fluctuations (2) factored in, respectively.

mated roughly according to delay time T_i of each station under the assumption of a plane time front; the position of the shower core ($X0$, $Y0$) is then determined by fitting pulse amplitudes A_i of each station with the Tunka fit function [9, 11]; the shower arrival direction is reconstructed more accurately under the assumption of a cone-shaped time front with the known position of the shower core; the energy is determined on the basis of the Q(200 m) value. Only the showers with cores located within the boundaries of the setup are selected for further study.

At the next stage, we use function (1) to approximate radial density $Q_i(R_i)$ of Cherenkov photons detected by station i and the corresponding dependence $A_i(R_i)$. It was demonstrated in [14, 15] that the positions of shower cores are determined accurately (with an error of ~1–3 m) by both the knee-like and Tunka fit functions if the number of triggered stations is sufficiently large ($N_{\rm hit} > 10$). Therefore, the standard procedure was used at the stage of core determination.

A total of 40 000 events in the 300–1000 TeV range with zenith angles below 25° and $N_{\rm hit} > 10$ were analyzed. The fit was very accurate for all events. Figure 2 shows two examples of experimental $Q(R)$ dependences and the corresponding fitting functions (1) on a log–log scale.

It can be seen that both types of LDFs (those with a sharp bend at the knee point and a dip in the central region and smooth LDFs) are approximated well. A considerable random spread of experimental points $Q_{\rm exp}$ about the fitting curve $Q_{\rm fit}$ is also seen. This spread is attributable to the possible errors of fitting and the inaccuracy of Q measurements (measurement fluctuations). It follows from general considerations that these fluctuations should be inversely proportional to the square root of Q, since Q is proportional to the number of detected photoelectrons. However, they may also depend on certain technical details of the measurement process. The distributions of deviations $d\log Q = \log Q_{\rm fit} - \log Q_{\rm exp}$ and $d\log A = \log A_{\rm fit} - \log A_{\rm exp}$ should be studied in order to construct a model of measurement fluctuations and introduce them into Monte Carlo simulations.

It was found (Fig. 3a) that $F(d\log Q)$ and $F(d\log A)$ in narrow Q (or A) intervals follow a Gaussian distribution with a root-mean-square deviation (RMS) decreasing rapidly with an increase in Q or A. The RMS(Q) and RMS(A) dependences were determined:

$$\begin{aligned} RMS(d\log Q) &= 0.092 - 0.059\log(Q[\text{Ch. Ph/cm}^2]) \\ RMS(d\log A) &= 0.02 - 0.033\log(A[\text{Ch. Ph/cm}^2]). \end{aligned} \quad (2)$$

The overall distribution of deviations was compared with the results of Monte Carlo modeling in CORSIKA 6990 for four types of particles: protons and helium, carbon, and iron nuclei. The energy spectrum of particles was a power-law one ($\sim E^{-1.67}$). Each one of the 28 stations measured the Q_i and A_i values, and measurement fluctuations with a Gaussian distribution and root-mean-square deviation (2) were added to them. The procedure of reconstruction of shower parameters (similar to the experimental one) was then applied. The events with $E = 300$–1000 TeV and zenith angles from 0° to 25° were selected. Figure 3b presents the comparison between the calculated and experimental functions $F(d\log Q)$ of the distribution of deviations from the fitting curve. It can be seen that they agree closely. These distributions do not follow the normal law.

The study of fluctuations is relevant for applications. As experience shows, they alter the fit parameters slightly and thus should be taken into account in

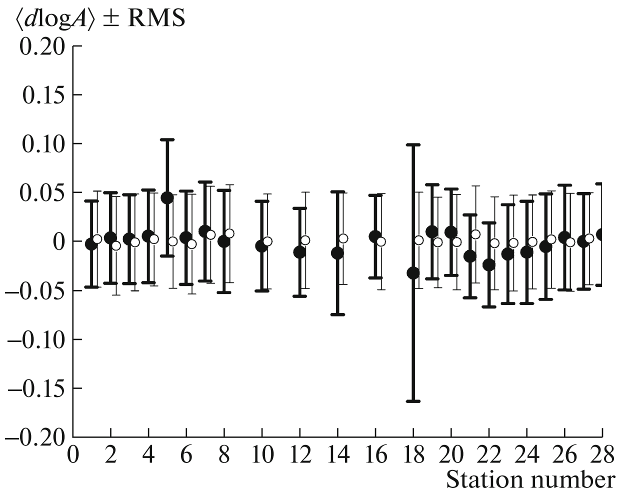

Fig. 4. Mean values of $d\log A$ and root-mean-square deviations from fitting functions for different stations obtained using the set of experimental events from January 1, 2017 (black dots). Gray dots represent the results of Monte Carlo modeling of events with measurement fluctuations (2) and errors that do not depend on the station number.

the parametric LDF analysis based on the comparison with Monte Carlo simulations.

4. EXAMPLES OF APPLICATION OF APPROXIMATIONS IN VARIOUS METHODOLOGICAL PROBLEMS

4.1. Performance Check for Optical Stations

Figure 4 shows the mean values and RMS of $d\log Q$ for different stations for the selection of experimental events and Monte Carlo simulations. It follows from the results of Monte Carlo modeling that neither the mean value nor the RMS should depend on the station number. In experiments, certain stations (nos. 14 and 18) have considerably larger RMS values, and certain stations (nos. 21–26) have a slight systematic shift of mean values. Performing this check for every day of observations, one may introduce corrections for each station.

4.2. Estimation of the Photon Density at an Arbitrary Point of the Setup Q(X, Y)

Owing to the high accuracy of fit, the knee-like approximation allows one to predict the density of Cherenkov photons at any fixed point of the setup. The first example is the estimation of Q_{200} (photon density at a distance of 200 m from the shower core in the shower plane). This quantity is almost proportional to energy and is used in HiSCORE to determine the energy. In our sample of experimental events (E = 300–1000 TeV, $\theta < 25°$, $N_{\rm hit} > 10$), the accuracy was determined in Monte Carlo simulations with measurement fluctuations (2) and was estimated at 5%.

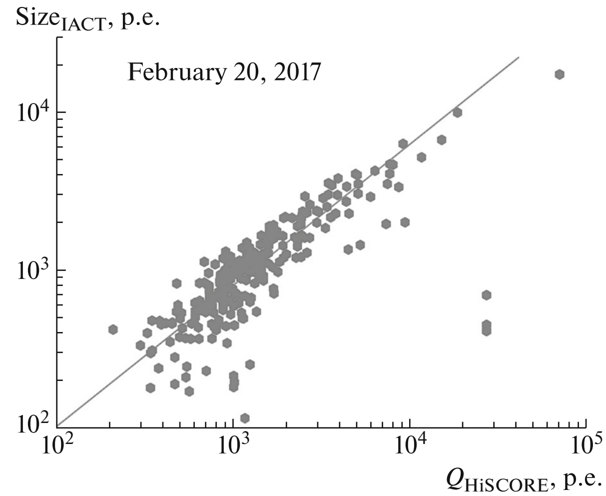

Fig. 5. IACT image size $Size_{\rm IACT}$ and the expected value derived from the HiSCORE data ($Q_{\rm HiSCORE}$).

The first IACT used in HiSCORE for gamma-ray astronomy was commissioned in 2017. It then became necessary to estimate the expected image size at the telescope position ($Q_{\rm HiSCORE}$) and compare it to the size measured by the IACT ($Size_{\rm IACT}$). The first data on the image sizes obtained at the commissioning phase (only 6 out of 34 mirrors were installed) are in good agreement (Fig. 5).

4.3. Comparison of the Accuracy of Fitting of the Same Set of Experimental LDFs by the Tunka and Knee-Like Functions

The $A(R)$ amplitude dependences were used. The root-mean-square error (RMSE) was calculated for each experimental event:

$$RMSE = \sqrt{\frac{\sum (d\log A_i)^2}{N}}, \quad (3)$$

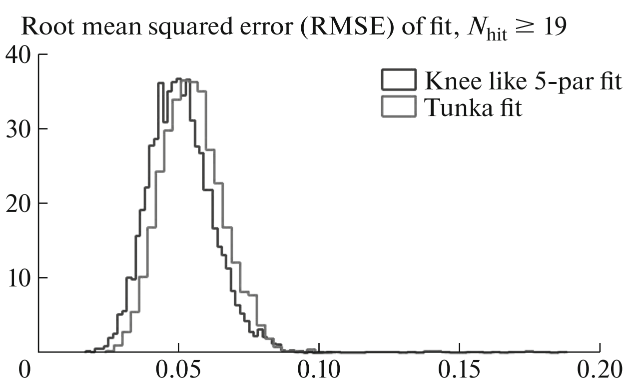

Fig. 6. RMSE (error of fitting of a single event) distributions of experimental events with different fitting functions: knee-like (left curve) and Tunka fit (right curve).

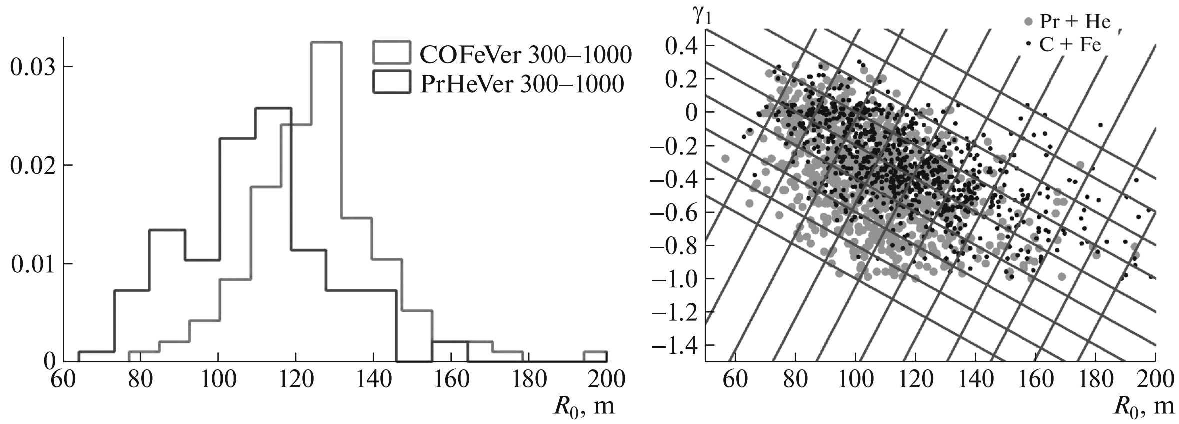

Fig. 7. Left panel: distribution of R_0 values; right panel: correlation between γ_1 and R_0. The data were obtained using simulated events for the groups of light (Pr + He) and heavy (C + Fe) nuclei in the 300–1000 TeV energy range at angles $\theta < 25°$.

where $d\log A_i = \log A_{\rm fit} - \log A_{\rm exp}$ are deviations of the experimental point from the fitting curve for station i, and N is the number of triggered stations minus two. The RMSE distribution of showers is shown in Fig. 6, where $\langle RMSE\rangle \sim 0.05$ for the knee-like fit and ~ 0.06 for the Tunka fit. The distributions are also similar in shape. As was mentioned in Section 1, much more significant differences are expected for distributions for certain types of events lacking in the sample under study (gamma-rays, events with larger angles, or events with lower energies).

4.4. Parameters Sensitive to the Depth of the Maximum

The most important objective of studies in the 300–1000 TeV range is the sorting of nuclei into different groups based on the LDF shape. The results of our Monte Carlo simulations revealed that parameter R_0, which depends linearly on the depth of the maximum (i.e., the distance to the EAS maximum), is the most sensitive. Parameters γ_1 and α also depend on the depth of the maximum. Figure 7 shows the distribution of R_0 and the scatter plot in coordinates $\gamma_1 - R_0$ for light (Pr + He) and heavy (C + Fe) groups of nuclei. The presented data were obtained in Monte Carlo simulations with the measurement fluctuations factored in. This problem requires multiparametric analysis and careful consideration of methodological issues and will be discussed in detail in further studies.

5. CONCLUSIONS

The application of knee-like approximations of the LDF of Cherenkov light, which were proposed earlier in [14–16], to real showers detected by TAIGA-HiSCORE in the 300–1000 TeV range was considered. Only the showers with well-measured (by ten or more stations) LDFs were examined. It was demonstrated that knee-like fitting functions are suitable for all varieties of LDFs of individual showers. The accuracy of fit is governed by fluctuations intrinsic to the process of measurement of the Cherenkov photon density. The probability density function of these fluctuations was estimated, and the dependence of the root-mean-square deviation on the photon density was determined. It was demonstrated that both of these laws should be taken into account in the comparison of experiments with Monte Carlo simulations. Several practical applications of knee-like approximations were considered: performance check for optical stations; cross calibration for the Cherenkov photon density measured by the IACT (image size) and HiSCORE stations; estimation of the accuracy of different approximations of photon density $Q(R)$ and density amplitude $A(R)$; analysis of the sensitivity of fitting parameters to the depth of the shower maximum and the particle type (this analysis is currently under way).

ACKNOWLEDGMENTS

This study was supported by the Russian Foundation for Basic Research (project no. 16-29-13035) and the Russian Science Foundation (project no. 15-12-20022, Sections 3 and 4). It was performed using facilities of the Common Use Center (CUC) of unique equipment under agreement no. 14.593.21.0005 with the Ministry of Science and Higher Education of the Russian Federation dated August 25, 2017.

REFERENCES

1. T. C. Weekes, M. F. Cawley, D. J. Fegan, et al., Astrophys. J. **342**, 379 (1989).
2. K. Meagher VERITAS Collab.), in *Proceedings of the 36th Cosmic Ray International Conference, July 30–Aug. 6, 2015, The Hague, Netherlands* (2016), p. 792.
3. J. Aleksić, J. High Energy Astrophys. **5–6,** 30 (2015). doi 10.1016/j.jheap.2015.01.002
4. A. Karle et al., Astropart. Phys. **3**, 321 (1995).

5. M. Tluczykont et al., Astropart. Phys. **56**, 42 (2014).
6. M. Tluczykont, D. Hampf, D. Horns, et al., Adv. Space Res. **48**, 1935 (2011).
7. L. Kuzmichev (TAIGA Collab.), EPJ Web Conf. **145**, 01001 (2017).
8. N. Budnev, et al., J. Phys.: Conf. Ser. **718**, 052006 (2016).
9. V. V. Prosin, S. F. Berezhnev, N. M. Budnev, et al., Nucl. Instrum. Methods Phys. Res., Sect. A **6**, 94 (2014).
10. V. V. Prosin, EPJ Web Conf. **99**, 04002 (2015).
11. E. Korosteleva et al., in *Proceedings of the 28th Cosmic Ray International Conference, July 31–Aug. 7, 2003, Tsukuba, Japan* (Universal Academy Press, Tokyo, 2003), p. 89.
12. J. R. Patterson and A. M. Hillas, J. Phys. G **9**, 1433 (1983).
13. S. Berezhnev et al., Nucl. Instrum. Methods Phys. Res., Sect. A **692**, 98 (2012).
14. A. Elshoukrofy, E. B. Postnikov, E. E. Korosteleva, L. G. Sveshnikova, and H. A. Motaweh, Bull. Russ. Acad. Sci.: Phys. **81**, 453 (2017).
15. A. Sh. M. Elshoukrofy et al., EPJ Web Conf. **145**, 19006 (2017).
16. A. Sh. M. Elshoukrofy, J. Phys.: Conf. Ser. **798**, 012184 (2017).
17. J. Hoerandel, Astropart. Phys. **199**, 193 (2003).

Translated by D. Safin